Journal of Power Sources 193 (2009) 930–934

Contents lists available at ScienceDirect

Journal of Power Sources

journal homepage: www.elsevier.com/locate/jpowsour

Short communication

Electrochemical behavior of carbon-nanotube/cobalt oxyhydroxide nanoflake multilayer films

Huajun Zheng[a,b,c], Fengqiu Tang[c], Melvin Lim[c], Thomas Rufford[c], Aniruddh Mukherji[c], Lianzhou Wang[c], Gaoqing (Max) Lu[c,*]

[a] Zhijiang College, Zhejiang University of Technology, Hangzhou 310024, PR China
[b] State Key Laboratory Breeding Base of Green Chemistry Synthesis Technology, Zhejiang University of Technology, Hangzhou 310014, PR China
[c] ARC Centre of Excellence for Functional Nanomaterials, School of Engineering and AIBN, The University of Queensland, St Lucia, Brisbane, QLD 4072, Australia

ARTICLE INFO

Article history:
Received 12 November 2008
Received in revised form 5 February 2009
Accepted 3 March 2009
Available online 14 March 2009

Keywords:
Multilayer film
Carbon nanotube
CoOOH nanoflake
Electrostatic self-assembly
Electrodeposition
Electrochemical capacitance

ABSTRACT

A new type of multilayer films consisting of multi-walled carbon nanotubes (MWCNTs) and cobalt oxyhydroxide nanoflakes (CoOOHNFs) are developed by alternately electrostatic self-assembly and electrodeposition technique, respectively. The successful growth of multilayer films composed of MWCNT and CoOOHNF are confirmed by scanning electron microscopy and X-ray photoelectron spectra. The multilayer film electrode is investigated for use in a supercapacitor with cyclic voltammograms and galvanostatic charge-discharge experiments. Experimental studies reveal that coatings of MWCNT/CoOOHNF on ITO glass present excellent electrochemical capacitance with specific capacitance being 389 F g^{-1}. The overall improved electrochemical behavior is accounted for the unique structure design in the multilayer films in terms of effective micro-porous nanostructure, large specific surface-area and good electrical conductance.

1. Introduction

Electrochemical capacitors (ECs), widely being used as power sources [1], have attracted much attention in current electrochemistry research because of their high energy densities and long cycle lives. The choice of material for use as electrodes is an important factor to improved-electrochemical capacitance because the performances of the ECs are highly dependent upon the nature of the electrode materials, such as compositions, structures and surface areas etc. Commonly, activated carbons with high surface areas were used as electrode materials for the electrochemical double layer capacitors; and transition-metal oxides were used as electrode materials for the pseudo-capacitors related to the redox reaction [2], respectively. Initially, RuO_2 generated great interest due to its high specific capacitance [3], but it has less possibility to be commercialized inmost applications because of its high cost. In attempting to develop economical electrodes, oxides of MnO_2 [4,5], Co_3O_4 [6], NiO_x [7], and SnO_2 [8] have been suggested for use.

Specifically, cobalt-based materials have been considered one of the most promising candidates for use in developing electrodes due to comparatively lower material costs. On the other hand, both their narrow potential-windows and relatively poorer electrochemical capacitances limit their possible usage in various applications. A key strategy to improving the electrochemical properties of such otherwise useful cobalt-based materials is the morphological and/or chemical composition design of cobalt-based materials at the nanometer-scale. Recently, nanostructured cobalt hydroxide $Co(OH)_2$ and cobalt oxyhydroxide (CoOOH) films as electrode materials were fabricated by the chemical-bath deposition [9–11] and electrodeposition methods [3] for the high-performance ECs which exhibited reasonably high pseudo-capacitance derived from the Co^{III}/Co^{II} redox process in aqueous solution. Other innovative methods include the addition of carbon nanotubes (CNTs) into transition-metal oxides (RuO_2, MnO_2, SnO_2-V_2O_5) to prepare multilayer film electrode materials [12–17], and the CNT used as substrates for the deposition of active materials [18,19]. These resultant multilayer film electrodes exhibited enhanced performances for ECs due to the advantages, such as highly accessible surface areas, high chemical stability, and good electrical conductivity [20,21].

The current work demonstrates the design of multilayer films consisting of multi-walled carbon nanotubes (MWCNTs) and cobalt oxyhydroxide nanoflakes (CoOOHNFs). The stepwise preparation firstly involves the electrostatic-assembly of well-dispersed carbon nanotubes on ITO glass followed by potentiostatically depositing CoOOHNF. Overall, this process leads to pronounced

* Corresponding author. Tel.: +61 7 33463828; fax: +61 7 33656074.
E-mail address: maxlu@uq.edu.au (G. Lu).

0378-7753/$ – see front matter © 2009 Elsevier B.V. All rights reserved.
doi:10.1016/j.jpowsour.2009.03.005

electrochemical performance and widened potential windows for pseudo-capacitors.

2. Experimental

2.1. Reagents and materials

The reagents and electrolytes, $CoCl_2{\cdot}6H_2O$, Na_2SO_4, NaOH, H_2SO_4, HNO_3, and Poly diallyl dimethyl ammonium (PDDA), were all of analytical grade (Aldrich Chemical Company, Inc.). Water was purified to a resistivity of 18.2 MΩ cm by passing through a Milli-Q water system. Indium-tin oxide (ITO)-coated glass (0.5 mm, 10 Ω cm^{-2}) was purchased from CSG Holding Co., Ltd, of Shenzhen, China. MWCNTs, with diameters 40-60 nm, were obtained from Shenzhen Nanotech Port Co. Ltd.

2.2. Oxidation and dispersion of MWCNT

Oxidation of MWCNT has been described in detail previously [22], Briefly, MWCNTs were oxidized by sonicatation in 20 ml of a mixture of H_2SO_4:HNO_3 (3:1) for 2 h, then washed using an aqueous NaOH solution. The oxidized-MWCNTs were sonicated, rinsed, and centrifuged, three times to obtain well-dispersed MWCNTs with negatively charged surfaces, and partially-oxidized carboxylic groups on the outer walls.

2.3. Preparation of the multilayer films of MWCNT and CoOOHNF

The multilayer films were fabricated on clean-ITO glass slides (the cleaning procedure is described in detail elsewhere [14–16]) via a two-step procedure as shown in Fig. 1. In the first step, the ITO substrate was dipped in a positively-charged PDDA polyelectrolyte solution (1 wt%, pH 11) containing 1.0 M NaCl, and submerged for 15 min, then rinsed with water and dried under a N_2 gas flow [23]. The positively charged PDDA-precoated substrate was subsequently placed horizontally in a solution of dispersed negatively-charged MWCNTs (0.5 mg dm^{-3}) for 30 min, rinsed with water, and dried with N_2 gas to deposit MWCNT layer on the substrate. After electrostatic absorbance of MWCNT layers, CoOOHNF were deposited by potentiostatic deposition from a solution of 0.05 M $CoCl_2$ at a potential of −1.0 V vs. Ag/AgCl, held for 30 min [24]. These two steps resulted in nanostructured multilayer films composed a bi-layer pair of MWCNT and CoOOHNF. The multilayer films with desired multiple layers of repeating MWCNT/CoOOHNF units were fabricated by repeating the electrostatic assembly and potentiostatic deposition for a number of cycles.

2.4. Multilayer film characterization

The topographical features of the films were examined by SEM (JEOL JSM-890). All samples were sputtered with platinum for 3 min before SEM observation to prevent charge accumulation. XPS analysis was performed on a Kratos Axis ULTRA X-ray Photoelectron Spectrometer using a monochromated Al Kα excitation source (1486.6 eV). The quantitative analysis was performed with CASAXPS software.

The mass of each layer (PDDA/MWCNT, or CoOOHNF) were obtained using the electrochemical quartz crystal microbalance (EQCM) technique. The quartz crystals used were commercially available 10 MHz, AT-cut type (diameter, 12.5 mm) consisted of 1000 Å Au with a 50 Å Cr under layer (Beijing Chenjing Electronic Co. Ltd). The frequency changes were measured by a PB-KIT-O1, EQCM-Pico balance measuring system (Technobiochip, S.C.AR.L., Italy). The EQCM device was placed in a static detection chamber with one quartz crystal exposed to a solution volume of 15.0 ml. When the coating deposited on the quartz crystal, the frequency response was stable within ±1.0 Hz over periods of 30 min. Base on the Sauerbrey equation, the mass of the assembly film was calculated by according to the frequency changes and linearly proportional between the frequency and the mass loading of the EQCM.

2.5. Electrochemical measurements

Electrochemical performance of the multilayer film electrodes was evaluated by cyclic voltammetry (CV) and galvanostatic charge-discharge cycles (GC) in a three-electrode electrochemical cell with the Solartron 1480A multistat. Platinum was used as the counter electrode, and Ag/AgCl as the reference electrode. The multilayer films on the ITO substrate as the working electrodes were dried at 120 °C under vacuum for 3 h prior to electrochemical measurements. The 0.1 M Na_2SO_4 electrolyte was degassed by bubbling with N_2 for 30 min to ensure the electrolyte was air-free. CV was measured at a scan rate of 10 mV s^{-1} and GC with a constant current of 1×10^{-5} A, over a cell potential window of 0.1 to 0.9 V.

The specific capacitance is used to evaluate quantitatively the capacitive properties of the multilayer film electrodes and obtained from the GC profiles:

$$SC = \frac{I \cdot \Delta t}{m \cdot \Delta V}$$

where SC is the specific capacitance of the multilayer film electrode (F g^{-1}); I is discharge current (in Fig. 6, $I = 1 \times 10^{-5}$ A); t is discharge time; ΔV is potential window (in this test, $\Delta V = 0.8$ V); m is the mass of the film deposited the PDDA/MWCNT layer or CoOOHNF layer. Base on the results of the EQCM method, the mass of PDDA/MWCNT and CoOOHNF layer are 1.10×10^{-6} and 2.27×10^{-6} g, respectively.

3. Results and discussion

3.1. Film characterization and multi-layer nanostructure

Fig. 2 presents the SEM images of the films of MWCNT and CoOOHNF deposited on the ITO glass substrates. In order to illuminate buildup of the multilayer films, the special surface section, which all of the substrate (ITO glass), MWCNT layer and CoOOHNF layer can be seen, was collected and the SEM image was showed as Fig. 2(A). From Fig. 2(A), it is observed that the MWCNT layer adsorbed on ITO glass slide and the CoOOHNF layer electrodeposited on the MWCNT layer. Fig. 2(B) shows an ITO glass slide deposited with (PDDA/MWCNT) clearly displaying a rough surface with randomly oriented MWCNT ranging from several hundred of nanometer to several micrometers in length. It also can be observed that the surface is densely covered with the CNT layer. Image shown in Fig. 2(C) is the surface morphology of the electrodeposition layer. It is apparent that a network of nanostructured flake is grown vertically on the surface of the CNT layer. The nanoflake

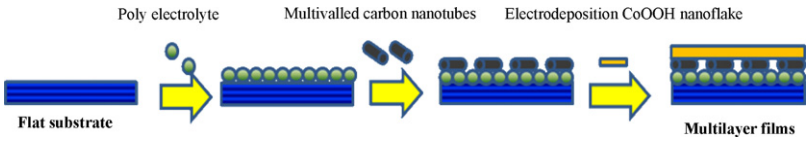

Fig. 1. Schematic illustration of preparation of the multilayer film.

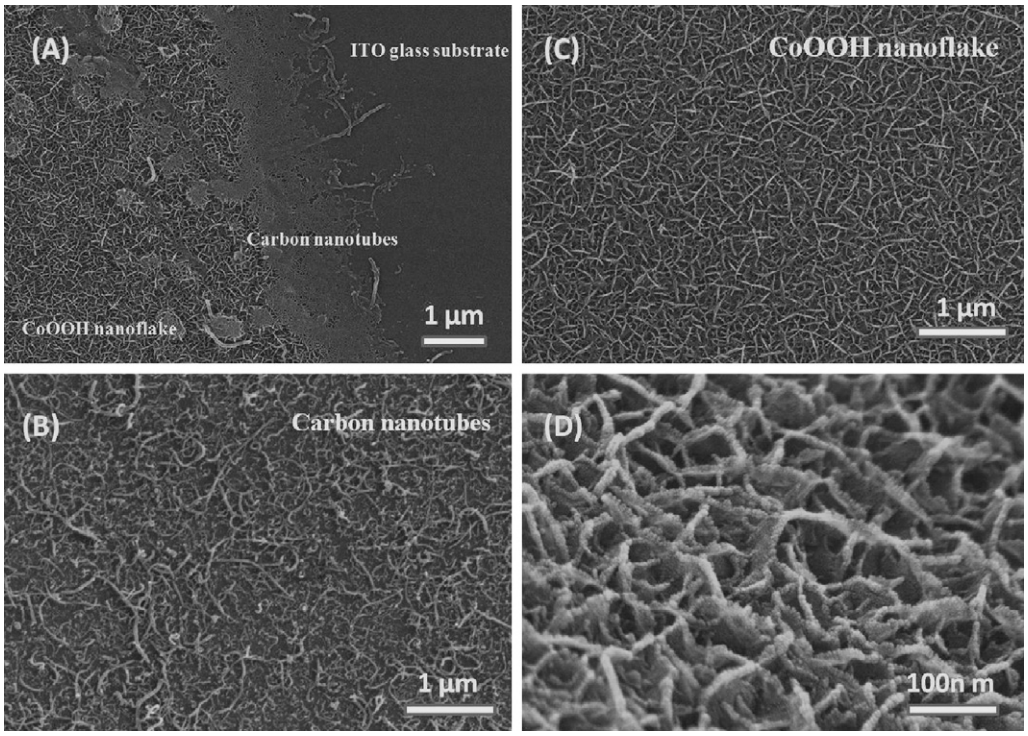

Fig. 2. SEM images of the multilayer film deposited on ITO glass substrate.

layer became more densely packed on the surfaces with the increase of electrodeposition time. A deposition time of 60 min led to the uniformly-coverage of the surface whereas a further increase of the deposition time had no apparent effect on morphology of the films. Fig. 2(D) is the high-magnification images with a tilting view of the electrodeposition layer. From Fig. 2(D), it is evident that the entire deposit consists of nanoflakes of individual size in the scale of hundreds of nanometers in length and ca. 10 nm in thickness, and the nanostructure is reticular layer with highly porous.

3.2. XPS surface analysis of the multilayer films

Fig. 3 shows the XPS survey scans of (1) ITO/MWCNT and (2) ITO/MWCNT/CoOOHNF samples. The peaks at 445.1 eV (In 3d), 486.0 eV (Sn 2p), and 525.7 eV (O 1 s) are associated with the InO_2 and SnO_2 of the ITO glass substrate, and these peaks are present for both ITO/MWCNT and ITO/MWCNT/CoOOHNF films. A peak assignable to C 1 s is centered at 285.0 eV in both spectra of Fig. 3. The high resolution XPS survey of this C1 s region, presented in Fig. 4(A), has an asymmetrical shape. This photoemission is characteristic of characteristic of CNT in a film [25].

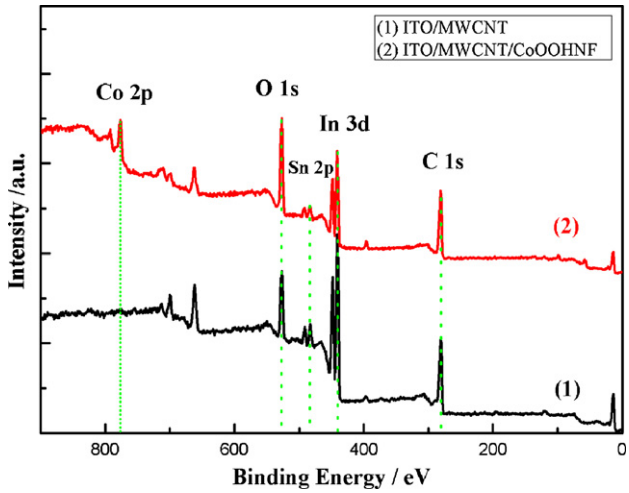

Fig. 3. XPS spectra for two type multilayer films (1) ITO/MWCNT and (2) ITO/MWCNT/CoOOHNF.

A Co (2p) peak appears only in the XPS survey scan of the ITO/MWCNT/CoOOHNF film. To check the chemical confirm the state of Co species, the high resolution XPS scan of the Co ($2p_{3/2}$) was calibrated for the In 3d (445.1 eV, with a full-width at half-maximum (FWHM) of 4.5 eV) and C1 s (285.0 eV with FWHM of 4.5 eV) associated with the ITO substrate. Deconvolution of the adjusted Co ($2p_{3/2}$) region, Fig. 4(B), shows an asymmetrical peak around 780.0 eV, attributed to Co^{III} species (i.e. CoOOH or hydrated Co_2O_3). Casella and Guascito [26] report that this peak is associated with the cobalt oxyhydroxide (CoOOH) species.

3.3. Electrochemical performances

Fig. 5 shows CV curves for (1) ITO/MWCNT, (2) ITO/CoOOHNF, and (3) ITO/MWCNT/CoOOHNF film electrodes in 0.1 M Na_2SO_4. The rectangular CV curve of ITO/MWCNT electrode is typical of reversible, double-layer capacitance. In contrast, the CV curve of ITO/CoOOHNF electrode has a broad current density peak from 0.42 V in the positive-charge sweep, and a peak from 0.84 V in the negative-charge sweeps, which are characteristic of pseudo-capacitance redox charge-transfer processes [27]. It can be seen clearly from curve 2 in Fig. 5 that ITO/CoOOHNF electrode shows relatively poorer pseudocapacitance properties and narrower potential with suitable windows in the range of 0.3–0.9 V. Fig. 5 shows the capacitive current of ITO/MWCNT/CoOOHNF film electrode is greater than that of ITO/MWCNT and ITO/CoOOHNF electrode. The potential window of ITO/MWCNT/CoOOHNF film electrode is larger, in the range of 0.1 to 0.9 V. This is evidence that carbon nanotubes contribute signifi-

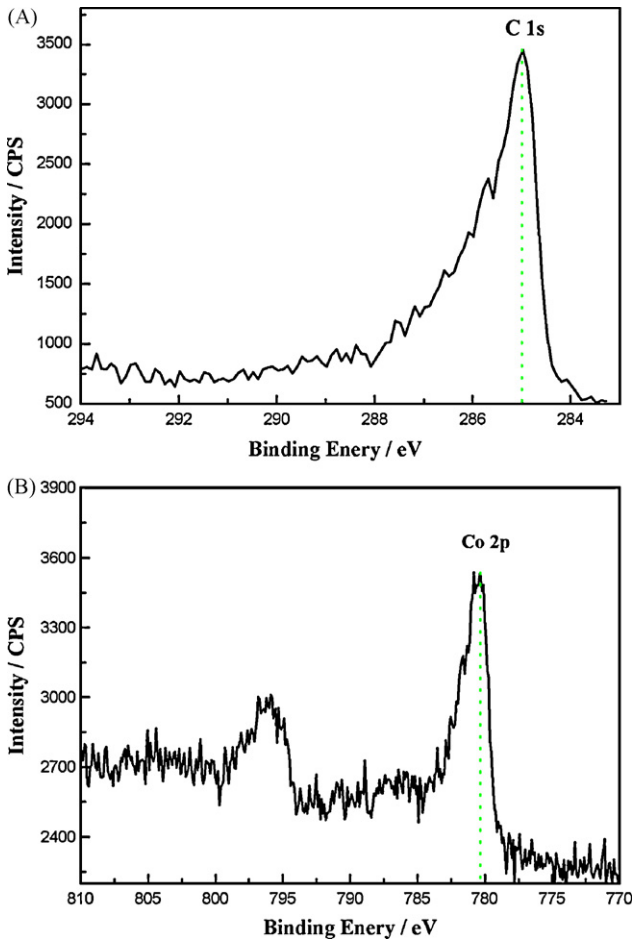

Fig. 4. High-resolution XPS of (A) the ITO/MWCNT for the C 1s region and (B) the ITO/MWCNT/CoOOHNF film for the Co 2p region.

cantly to the enhanced capacitance of the multilayer film electrode. The CV curves of ITO/MWCNT/CoOOHNF film electrode feature both electric double-layer capacitance and pseudo-capacitance characteristics: the MWCNT layer provides an increased surface area/porous structure for double-layer capacitance and the CoOOHNFs layer provide pseudo-capacitance from Co^{III}/Co^{II} redox process. In other words, electric double-layer capacitance and

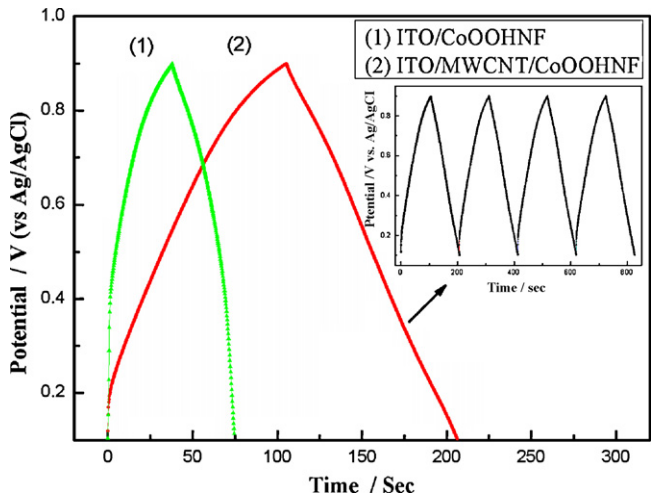

Fig. 6. Chronopotentiograms of the multilayer film electrodes (1) ITO/CoOOHNF; (2) ITO/MWCNT/CoOOHNF at charge-discharge current density of 1×10^{-5} A cm^{-2} in 0.1 M of Na_2SO_4 electrolyte. The Insert is GC of the ITO/MWCNT/CoOOHNF film electrode for four charge-discharge cycles.

pseudo-capacitance are both interfacial phenomena which take place in the ITO/MWCNT/CoOOHNF film electrode.

GC charge-discharge profiles of electrodes prepared with repeated MWCNT/CoOOHNF layers are shown in Fig. 6. The single-electrode specific capacitance, SC, was calculated from the GC profiles. We observe that SC of the ITO/MWCNT/CoOOHNF (389 F g^{-1}) film electrode is more than that of the ITO/CoOOHNF (209 F g^{-1}) electrode, which shows the CNT layer plays a significant role in enhancing the capacitance of the multilayer film electrode. Because CoOOHNF layer is deposited onto the randomly distributed MWCNT layer with a unique porous structure, the ITO/MWCNT/CoOOHNF film for electrochemical capacitors possessing a high specific surface area can expand the charge-storage capacity. Such porous structures of MWCNT/CoOOHNF film are beneficial to the transportation of electrolyte ions, and the insertion and removal of H^+ or OH^- resulted from the reactions, which owes a great deal to the much more full utilization of the electroactive material. It is natural that the obtained high SC of 389 F g^{-1} from the synthesized ITO/MWCNT/CoOOHNF film electrode is mainly attributed to the effective porous nanostructure and high specific surface area.

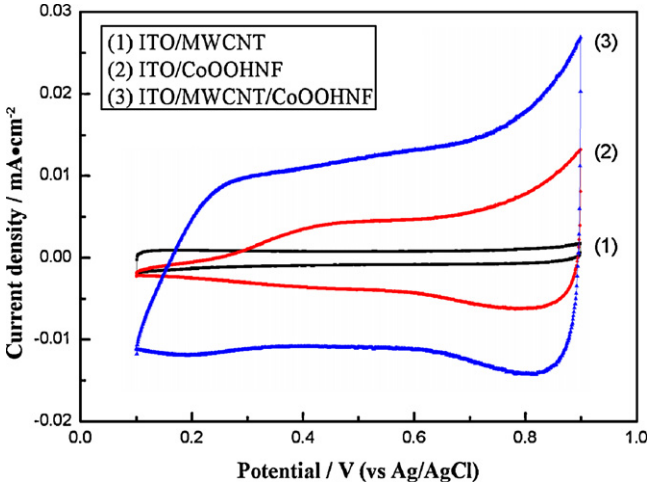

Fig. 5. CV of various multilayer film electrodes (1) ITO/MWCNT; (2) ITO/CoOOHNF and (3) ITO/MWCNT/CoOOHNF in 0.1 M of Na_2SO_4 electrolyte at scan rate of 10 mV s^{-1}.

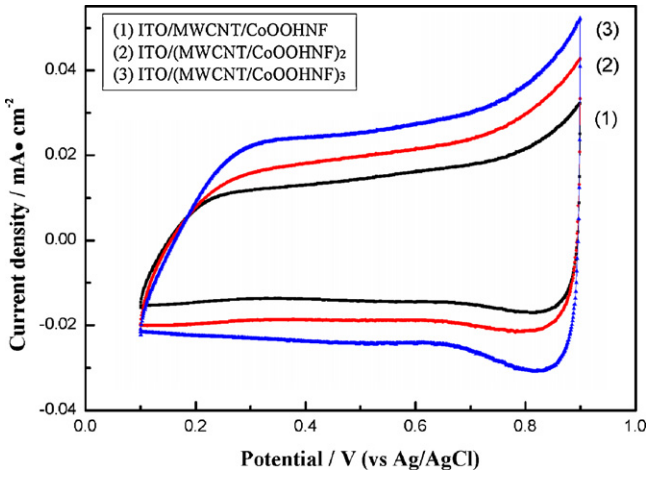

Fig. 7. CV of various multilayer film electrodes (1) ITO/MWCNT/CoOOHNF; (2) ITO/(MWCNT/CoOOHNF)$_2$ and (3) ITO/(MWCNT/CoOOHNF)$_3$ in 0.1 M of Na_2SO_4 electrolyte at scan rate of 10 mV s^{-1}.

Another important aspect of the multilayer film electrode is the progressive enhancement of specific capacitance with increasing the (MWCNT/CoOOHNF) pair numbers. The SC of the ITO/(MWCNT/CoOOHNF)$_2$ and the ITO/(MWCNT/CoOOHNF)$_3$ film electrodes are 586 and 802 F g^{-1}. Similar conclusion was obtained from Fig. 7, the box area of CV curve of ITO/(MWCNT/CoOOHNF)$_3$ film electrode is much larger than ITO/(MWCNT/CoOOHNF)$_2$ film electrode, and the area of CV curve of ITO/(MWCNT/CoOOHNF)$_2$ film electrode is also larger than ITO/MWCNT/CoOOHNF film electrode. This is a merit for this new type of multilayer film, which further improvement in electrochemical capacity may be achieved by optimized assembly of the MWCNT/CoOOHNF units.

4. Conclusions

A new type of multilayer film composing of MWCNT and CoOOHNF were synthesised using electrostatic assembly and potentiostatically deposition, in a step-wise coating process. The ITO/MWCNT/CoOOHNF film electrodes present better electrochemical properties than the ITO/CoOOHNF and ITO/MWCNT electrodes. The MWCNT layer provides a large surface area for the dispersion of CoOOHNF, and also improves the electrical conductivity of the film. Electrochemical capacitors fabricated with the ITO/MWCNT/CoOOHNF film electrode produced a high SC of 389 F g^{-1}. A progressive enhancement in SC is observed with increasing the number of (MWCNT/CoOOHNF) layers. It is foreseen that these multilayer film electrodes are important in aiding the development of highly efficient electrochemical capacitors in the near future.

Acknowledgments

This work was financially supported by the Zhejiang Natural Science Foundation (No.Y4080042) and the Australian Research Council's Centre of Excellence Program. Huajun Zheng is grateful for the financial support from the China Scholarship Council (CSC).

References

[1] J.H. Sung, S.J. Kim, S.H. Jeong, E.H. Kim, K.H. Lee, J. Power Sources 162 (2006) 1467–1470.
[2] J. Chmiola, G. Yushin, Y. Gogotsi, C. Portet, P. Simon, P.L. Taberna, Science 313 (2006) 1760–1763.
[3] V. Gupta, T. Kusahara, H. Toyama, S. Gupta, N. Miura, Electrochem. Commun. 9 (2007) 2315–2319.
[4] T. Xue, C.L. Xu, D.D. Zhao, X.H. Li, H.L. Li, J. Power Sources 164 (2007) 953–958.
[5] K.R. Prasad, N. Miura, J. Power Sources 135 (2004) 354–360.
[6] Y. Shan, L. Gao, Mater. Chem. Phys. 103 (2007) 206–210.
[7] Y.G. Wang, Y.Y. Xia, Electrochim. Acta 51 (2006) 3223–3227.
[8] K.R. Prasad, N. Miura, Electrochem. Commun. 6 (2004) 849–852.
[9] H.J. Ahn, W.B. Kim, T.Y. Seong, Electrochem. Commun. 10 (2008) 1284–1287.
[10] E. Hosono, S. Fujihara, I. Honma, M. Ichihara, H. Zhou, J. Power Sources 158 (2006) 779–783.
[11] C. Yuan, X. Zhang, B. Gao, J. Li, Mater. Chem. Phys. 101 (2007) 148–152.
[12] J.H. Park, J.M. Ko, O.O. Park, J. Electrochem. Soc. 150 (2003) A864–867.
[13] Y.T. Wu, C.C. Hu, J. Electrochem. Soc. 151 (2004) 2060–2066.
[14] G.X. Wang, B.L. Zhang, Z.L. Yu, M.Z. Qu, Solid State Ionics 176 (2005) 1169–1174.
[15] C.Y. Lee, H.M. Tsai, H.J. Chuang, S.Y. Li, P. Lin, T.Y. Tseng, J. Electrochem. Soc. 152 (2005) A716–A720.
[16] Z. Fan, J.H. Chen, M.Y. Wang, K.Z. Cui, H.H. Zhou, Y.F. Kuang, Diamond Relat. Mater. 15 (2006) 1478–1483.
[17] M. Jayalakshmi, M.M. Rao, N. Venugopal, K.B. Kim, J. Power Sources 166 (2007) 578–583.
[18] S.B. Ma, K.Y. Ahn, E.S. Lee, K.H. Oh, K.B. Kim, Carbon 45 (2007) 375–382.
[19] E.H. Liu, X.Y. Meng, R. Ding, J.C. Zhou, S.T. Tan, Mater. Lett. 61 (2007) 3486–3489.
[20] A.K. Chatterjee, M. Sharon, R. Banerjee, M. Neumann-Spallart, Electrochim. Acta 48 (2003) 3439–3446.
[21] C. Li, D. Wang, T. Liang, X. Wang, L. Ji, Mater. Lett. 58 (2004) 3774–3777.
[22] H.J. Zheng, F.Q. Tang, Y. Jia, L.Z. Wang, Y.C. Chen, M. Lim, L. Zhang, G.Q. (Max) Lu, Carbon, (2009), doi:10.1016/j.carbon.2009.02.004.
[23] M.A. Corra-Duarte, A. Kosiorek, W. Kandulski, M. Giersig, L.M. Liz-Marza, Chem. Mater. 17 (2005) 3268–3272.
[24] Q. Nguyen, L.Z. Wang, G.Q. Lu, Int. J. Nanotechnol. 4 (2007) 585.
[25] E.S. Henriette, Carbon 42 (2004) 1713–1721.
[26] I.G. Casella, M.R. Guascito, J. Electroanal. Chem. 476 (1999) 54–63.
[27] V. Srinivasan, J.W. Weidner, J. Power Sources 108 (2002) 15–20.